

Dynamic Causal Modeling of Insular, Striatal, and Prefrontal Cortex Activities During a Food-Specific Go/NoGo Task

Qinghua He, Xiaolu Huang, Shuyue Zhang, Ofir Turel, Liangsuo Ma, and Antoine Bechara

ABSTRACT

BACKGROUND: This study aimed to investigate the dynamic interactions among three neural systems that are implicated in substance and behavioral addictions in response to food cues in young adults. These include an impulsive system involving the striatum, a reflective system involving the prefrontal cortex, and a homeostasis sensing system involving the insular cortex.

METHODS: College students ($N = 45$) with various levels of body mass index were recruited. Functional magnetic resonance imaging data were acquired while participants performed food-related Go/NoGo tasks, with low-calorie and high-calorie food cues. Participants were scanned under both food satiety and deprivation conditions. Dynamic causal modeling was applied to the data to examine the causal architecture of coupled or distributed dynamics among the aforementioned systems.

RESULTS: Participants showed difficulty inhibiting responses to high-calorie foods as suggested by higher false alarm rate and decision bias for low-calorie food Go task. This difficulty was enhanced during the food deprivation condition. Deprivation increased neural activity of both the insula and the striatum bilaterally in response to high-calorie foods during Go trials and anterior cingulate cortex and dorsolateral prefrontal cortex activity during NoGo trials. Dynamic causal modeling analysis revealed that food deprivation modulated the communications between the insula, striatum, and dorsolateral prefrontal cortex, and the modulations were positively associated with body mass index.

CONCLUSIONS: The results support tripartite views of decision making. Deprivation states, such as hunger, trigger insular activity, which modulates the balance between impulsive and reflective systems when facing tempting food cues.

Keywords: Deprivation, Dorsolateral prefrontal cortex, Dynamic causal modeling, fMRI, Food, Insula, Striatum

<https://doi.org/10.1016/j.bpsc.2018.12.005>

Food is very important for human survival. Nevertheless, overconsumption of food can lead to overweight and obesity, which have become a key global public health concern (1–3) because they are associated with increased risk for cardiovascular and metabolic diseases as well as several types of cancer in adults (4). Research on excess weight gain has been dominated by a focus on underlying metabolic mechanisms (5). The question of why people decide to eat unhealthy foods that drive excess weight gain in the first place, that is, viewing excess weight gain as partially associated with food choice decisions, is relatively newer and has been relatively understudied. Taking this perspective, several studies have suggested that the difficulty to resist unhealthy foods is subserved by alterations in neural systems implicated in impaired decision making and behavioral addictions (6–11). The studies suggest that an individual who persistently chooses to eat high-calorie foods, despite the risk of potential long-term negative consequences of excess weight, may be similar to someone who is addicted to other substances or behaviors in terms of

underlying brain mechanisms; they are simply drawn to immediate food rewards, while ignoring long-term adverse consequences (6).

Adapting this behavioral addiction view, we contend that the loss of willpower to resist the temptation of high-calorie food and the development of eating habits that lead to excess weight may be explained in part in terms of abnormal activity in any one or a combination of three key neural systems that underlie addiction development and maintenance (12). These include 1) an impulsive system involving the striatum that drives reward seeking, 2) a reflective system involving the prefrontal cortex (PFC) that exerts self-control, and 3) an interoceptive awareness/homeostasis sensing system involving the insular cortex (i.e., the insula) that responds to deprivation states (e.g., hunger) and consequently alters the dynamics of the impulsive and reflective systems. It does so by intensifying impulsive system activity and reducing reflective system activity. Specifically, individuals with addictive disorders often have a hyperactive

impulsive system that promotes automatic, habitual reward-seeking behaviors (3,13–16) and show higher levels of impulsivity (17–20). They also can have a hypoactive reflective system, which hinders their impulse control capacities and the ability to resist stimuli that are rewarding in the short term but lead to negative consequences in the long term (3,12–14). They show loss of cognitive control over addiction cues, and this may be modulated by reduced striatal dopamine D₂ receptor (21,22). The insular cortex system is very sensitive to the sense of body (17,23–26). In addictive disorders, it translates homeostatic and interoceptive signals triggered by states of deprivation, or by exposure to reward cues (e.g., high-calorie food cues), into craving and what may become subjectively experienced as an urge to generate the reward via the behavior that produces it (e.g., eat the food) (27). Consistent with this perspective, a rising number of studies suggest that these same brain regions that have been implicated in substance and behavioral addiction research have altered responses to food cues in overweight and obese individuals (6–11).

The present study aimed to investigate the neural dynamics among these three neural systems in response to food cues in young adults. To do so, participants were scanned twice: 1) under a food satiation condition and 2) under a food deprivation condition. We used a food-related Go/NoGo task with low-calorie and high-calorie food cues and then applied a dynamic causal modeling (DCM) analysis to the data (28) to examine the causal architecture of coupled or distributed dynamics of central brain regions of the impulsive, reflective, and interoceptive brain systems. Consistent with theoretical dynamics portrayed in neural models of addictive behaviors (12) and the view that excess weight may be associated in part with deficits in systems that govern decision making (3), we tested the hypotheses that 1) food deprivation states engage the insula, which, in turn, 2)

exacerbates the activity of the impulsive system and 3) weakens activity of the control function of the reflective system. Consistent with the view of excess weight as stemming in part from decision-making deficits (3), we also expected that these effects would be positively associated with body mass index (BMI).

METHODS AND MATERIALS

Participants

We recruited 45 volunteers (28 women; mean age 20 ± 1.1 years; age range, 18–22 years) from the University of Southern California. Participants with neurologic or psychiatric disorders were excluded (see Supplement for details). All participants gave informed consent to the study procedures, which were approved by the University of Southern California Institutional Review Board.

Procedures

Participants were asked to come to the laboratory for three sessions (Figure 1A). During the first visit, participants were asked to complete and sign the consent form and complete the screening interview and behavioral tasks. Participants were then scheduled to return for two functional magnetic resonance imaging (fMRI) scans on two different dates: one in a food satiated (full) condition and another in a food deprived (hunger) condition. Right before each fMRI session, their height and weight were measured, and a 24-hour dietary recall was conducted with the Nutrition Data System for Research (NDSR). During each session, participants completed two versions of the food-specific Go/NoGo task (8 minutes each) and one structural scan for registration purposes; these lasted about 35 minutes.

Under the satiation condition, participants were asked to eat normally and to have their usual meal right before they arrived

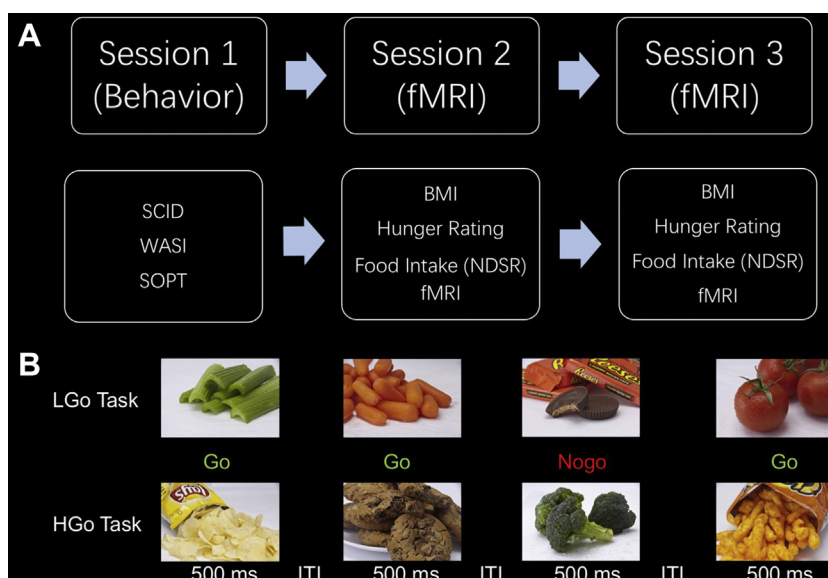


Figure 1. Design of the study. **(A)** Schematic of the procedure. Participants were asked to visit the laboratory for three sessions: one behavioral session, and two functional magnetic resonance imaging (fMRI) sessions (one under satiated/full condition, the other under deprived/hunger condition). The order of the two fMRI sessions was counterbalanced across participants. Participants who were scanned under the satiated/full condition were asked to eat normally and to have their usual meal before they arrived for the fMRI session. For the food deprived/hunger condition, participants were asked refrain from eating from 8 PM the day before the scan. **(B)** Illustration of the event-related food-specific Go/NoGo tasks: low-calorie food Go/high-calorie food NoGo (LGo) task and high-calorie food Go/low-calorie food NoGo (HGo) task. Participants were asked to press a button as soon as possible to the Go trials (vegetable pictures in LGo task and snack pictures in HGo task) and withhold the response to the NoGo trials (snack pictures in LGo task and vegetable pictures in HGo task). The order of tasks was counterbalanced across subjects. BMI, body mass index; ITI, intertrial interval; NDSR, Nutrition Data System for Research; SCID, Structured Clinical Interview for DSM-IV; SOPT, self-ordered pointing task; WASI, Wechsler Abbreviated Scale of Intelligence.

Nutrition Data System for Research; SCID, Structured Clinical Interview for DSM-IV; SOPT, self-ordered pointing task; WASI, Wechsler Abbreviated Scale of Intelligence.

for the fMRI session. They were asked to eat a variety of snacks (such as crackers and chocolate) provided to them until they felt full at the laboratory. For the food deprivation condition, participants were asked to refrain from eating starting at 8 PM on the day before the scan. All scans were scheduled in the morning between 10 AM and 11 AM to avoid variation of scanning time and potential development of hunger. For manipulation-check purposes, participants were asked to rate their hunger levels on a scale of 1 (not hungry at all) to 10 (very hungry) right before the scan. The satiation and deprivation sessions were counterbalanced across participants, and they were separated by more than 30 days (on average 41.2 ± 7.3 days; range, 33–52 days) to avoid practice effects. The time between the scans did not correlate with either session or BMI (both $p > .05$).

Measures

Neuropsychological Assessment. Participants were asked to complete two behavioral tasks (Table 1). The Wechsler Abbreviated Scale of Intelligence (29) was used as an estimate for IQ, and the self-ordered pointing task (30) was used as an index of working memory and executive function.

Dietary Intake. A single, in-person 24-hour dietary recall was conducted by trained research staff using a multipass method facilitated by the NDSR (31,32). Details of the NDSR procedure can be found in the Supplement. The software calculated low-calorie and high-calorie food consumption (servings per day), which served as the dietary intake index in the present study.

Food-Specific Go/NoGo Tasks

Using a different cohort of participants from He *et al.* (14), participants performed two event-related food-specific Go/NoGo tasks adapted from He *et al.* (14) in each scan: 1) a low-calorie food Go/high-calorie food NoGo task and 2) high-calorie food Go/low-calorie food NoGo task. The only difference from He *et al.* (14) is that in the current study, participants were scanned twice, several weeks apart. A detailed description of these tasks is presented in the Supplement. Figure 1B shows a sample of food pictures.

The hit rate, false alarm rate, sensitivity index, and decision bias were calculated for each task following prior research with the same paradigm (14,33). The mean reaction time for Go trials and NoGo trials (false alarm trials only) for each task was also calculated. The reaction time for Go trials served as an index for automatic responding to the stimuli, with longer reaction times indicating less habitual responses; decision bias

served as an index of response inhibition, with higher values indicating better inhibitory control.

fMRI Data Analysis

Participants finished two runs of Go/NoGo tasks in each scanning session. Details of fMRI data acquisition and pre-processing are presented in the Supplement. Univariate fMRI data were modeled using a general linear model by convolving the onsets of each condition with the canonical hemodynamic response function. There were eight conditions in the first level model, representing each cell in the 2 condition (satiated vs. deprived) \times 2 task (Go vs. NoGo) \times 2 stimuli (low-calorie vs. high-calorie food cues) within-subject factor design. Statistical significance was defined as cluster-forming threshold at $p < .001$ and familywise error-corrected cluster threshold at $p < .05$. Behavior and brain data correlation was calculated using robust correlation, and Bonferroni corrections were applied to adjust for familywise error.

Stochastic DCM

DCM with DCM12 (revision 6906) was used for connectivity analysis. DCM is described in detail elsewhere (28). In brief, it develops a biophysical model of the underlying neuronal connectivity and how the neuronal connectivity generates the observed blood oxygen level-dependent signal. The DCM analysis included three regressors: 1) habitual response manifested in onsets of all Go trials, 2) reflective response manifested in onsets of all NoGo trials, and 3) deprivation response onsets of all trials under deprivation condition.

Regions of interest were regions that met all the following criteria: 1) showed significant activation in the univariate second-level analysis; 2) showed activation in previous fMRI studies using Go/NoGo tasks (34,35); and 3) had a theoretical reason to be activated as per the tripartite model of addictive behaviors (12,27,36). Eight nodes (Supplemental Figure S1) met these criteria and were consequently used in the DCM analyses: 1) left insula, 2) right insula, 3) ventromedial PFC (VMPFC), 4) anterior cingulate cortex (ACC), 5) left striatum, 6) right striatum, 7) left dorsolateral PFC (DLPFC), and 8) right DLPFC.

Volumes of interest (VOIs) were obtained by significant activation clusters, which were determined by second-level random effects univariate analysis. Cluster maxima locations were used as VOI centers around which 6-mm spheres were extracted as the VOI regions. The standard SPM procedure was followed by using the principal eigenvariate of each VOI as a summary of the functional activity time series in that VOI (37), and each principal eigenvariate time series was adjusted for

Table 1. Descriptive Statistics in the Two Sessions

	Satiation Session	Hunger Session	<i>t</i> (<i>df</i>)	<i>p</i>
BMI	22.9 \pm 3.5 (19.1–33.7)	22.8 \pm 3.0 (18.5–31.3)	0.46 (44)	.65
Hunger Rating	2.5 \pm 2.0 (1–5)	6.6 \pm 1.9 (6–10)	–2.86 (44)	< .01
NDSR Low-Calorie Foods	2.7 \pm 1.7 (0.3–7.5)	2.8 \pm 1.5 (0.3–5.4)	–0.30 (44)	.77
NDSR High-Calorie Foods	1.9 \pm 1.5 (0.0–5.7)	1.8 \pm 1.5 (0.0–6.0)	0.82 (44)	.42

Values are presented as mean \pm SD (range).

BMI, body mass index; NDSR, Nutrition Data System for Research.

the F-contrast of effects of interest (38). The same VOIs were used across subjects.

DCM structure inference was conducted using DCM network discovery (39). Before the DCM network discovery analysis was conducted, a single full model was specified for each subject. Group-level post hoc optimization was conducted by selecting all inverted full models (one per subject). The optimal sparse model was found at the group level by using Bayesian parameter averaging. The correlation of behavioral and DCM data was calculated using the robust correlation.

RESULTS

Behavioral Results

The average IQ of our sample was normal (mean = 118.4, SD = 9.8, range = 103–136), and the executive function performance was normal according to the self-ordered pointing task (mean = 65.1, SD = 3.8, range = 56–70). Descriptive statistics regarding BMI, hunger rating, and food intake are presented in Table 1. Only hunger ratings significantly differed between the two sessions; in support of intervention validity, $\text{hunger}_{\text{deprived}} > \text{hunger}_{\text{satiated}}$.

Food Go/NoGo task behavior measures were analyzed with 2 condition (satiated vs. deprived) \times 2 task (high-calorie food Go/low-calorie food NoGo task vs. low-calorie food Go/high-calorie food NoGo task) within-subject analysis of variance (Supplemental Table S1). After Bonferroni correction, only two main effects of task were significant: on 1) false alarm: $F_{1,42} = 11.46, p = .002$, partial $\eta^2 = .42$, and on 2) decision bias: $F_{1,42} = 9.89, p = .003$, partial $\eta^2 = .45$, suggesting that in the high-calorie food Go/low-calorie food NoGo task, participants had smaller false alarm rate and higher inhibition control (decision bias) than in the low-calorie food Go/high-calorie food NoGo task. We also found a significant main effect of task on reaction time in Go trials ($F_{1,42} = 4.89, p = .03$, partial $\eta^2 = .23$) and a significant effect of condition on reaction time in NoGo trials

($F_{1,42} = 5.24, p = .03$, partial $\eta^2 = .32$). However, these effects were not sustained after multiple comparison correction.

fMRI Univariate Analysis

fMRI second-level random effects one-sample *t* test analyses revealed several statistically significant clusters for main effects and interactions (Table 2 and Figure 2). They suggested that 1) the left and right insula were significantly activated in deprivation versus satiation conditions; 2) the ACC, left DLPFC, and right DLPFC showed more activation in NoGo trials compared with Go trials; 3) the left and right striatum showed significant activation in interaction between task and stimuli versus baseline; and 4) the VMPFC showed significant activation in the three-way interaction versus baseline.

The percent signal change of the significant clusters showing interaction effects were extracted and plotted for different groups (Figure 3). Further analysis showed that left (Figure 3A) and right (Figure 3B) striatum were more highly activated in Go trials of high-calorie food than in low-calorie food trials (all $t > 3.23, p < .001$), but this difference was not present in the NoGo trials ($p > .05$). The VMPFC (Figure 3C) showed higher activity in low-calorie food Go trials than in high-calorie food trials. It also showed higher activity in high-calorie food NoGo trials than in low-calorie food trials. This difference was present during the satiation condition (both $t > 3.58, p < .001$) but not in the deprivation condition ($p > .05$).

The extracted percent signal changes were also correlated with BMI and NDSR scores. To reduce the number of multiple comparisons, the left and right striatum, the ACC and right DLPFC, and the left and right insula were linearly paired. The two sessions of NDSR and BMI scores were also combined. Results suggest that striatal activity when a person sees high-calorie foods in the Go trials, under either satiation or deprivation condition, correlated positively with NDSR high-calorie foods (satiation: $r_{45} = .528, p < .001$; deprivation: $r_{45} = .623, p < .001$) and BMI (satiation: $r_{45} = .453, p < .002$; deprivation:

Table 2. Summary of Univariate fMRI Results

L/R	Brain Region	Voxels	MNI			F	p
			x	y	z		
Main Effect of Condition (Hungry > Satiated)							
R	Insula	132	33	20	-7	22.11	< .001
L	Insula	124	-39	14	-7	19.45	< .001
Main Effect of Task (NoGo > Go)							
R	DLPFC	503	30	20	20	20.46	< .001
L/R	ACC	254	6	20	23	18.79	< .001
L	DLPFC	100	-45	35	23	18.22	< .001
Interaction Between Task and Stimuli							
L	Putamen/striatum	107	-30	-13	-7	19.02	< .001
R	Putamen/striatum	103	33	2	-1	18.58	< .001
Three-Way Interaction (Task \times Stimuli \times Condition)							
L/R	VMPFC	159	-9	47	-16	19.11	< .001

The voxel size in fMRI analysis is 2 mm \times 2 mm \times 2 mm = 8 mm³. The x, y, and z coordinates and the *F* and *p* values were reported on the peak voxel.

ACC, anterior cingulate cortex; DLPFC, dorsolateral prefrontal cortex; fMRI, functional magnetic resonance imaging; L, left; MNI, Montreal Neurological Institute; R, right; VMPFC, ventromedial prefrontal cortex.

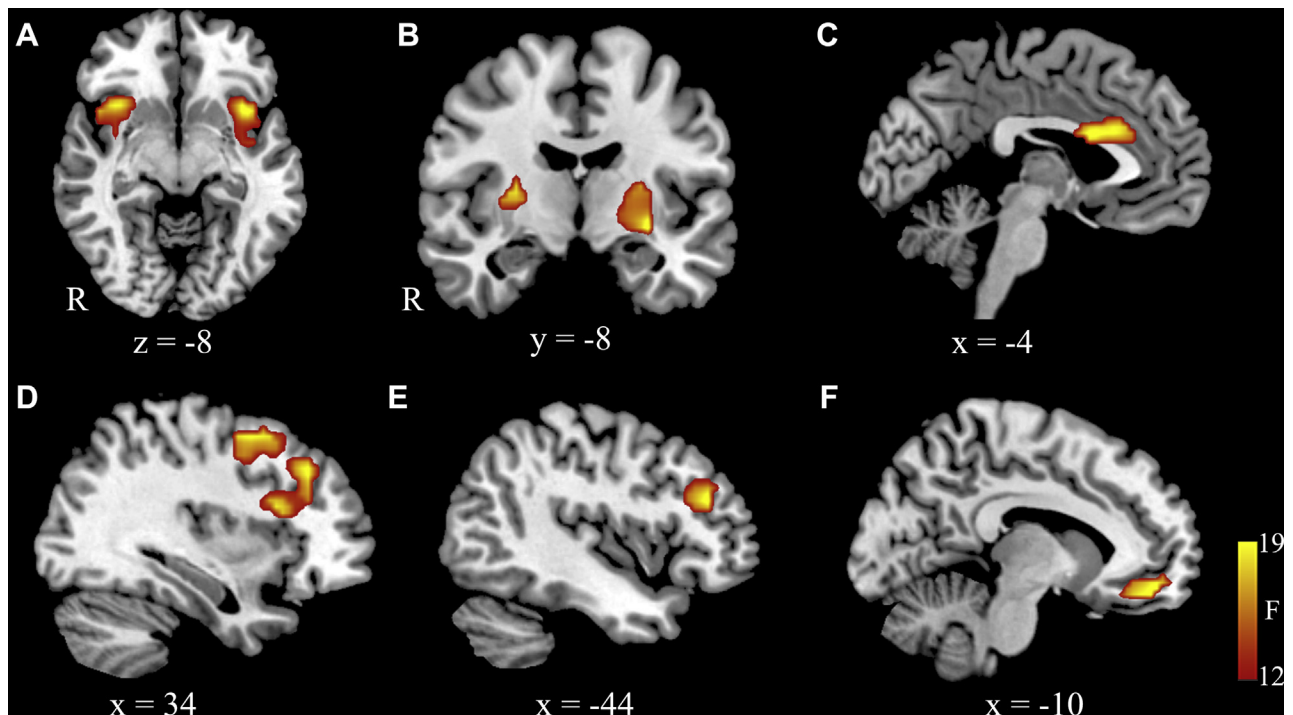


Figure 2. Univariate two-way functional magnetic resonance imaging analysis of variance results. (A) Left and right insula showed significant activation in main effect of condition. (B) Left and right striatum showed significant activation in interaction between task and stimuli. The main effect of task showed activation in the anterior cingulate cortex (C), left dorsolateral prefrontal cortex (D), and right dorsolateral prefrontal cortex (E). (F) The ventromedial prefrontal cortex showed significant activation in the three-way interaction. R, right hemisphere.

$r_{45} = .578, p < .001$). The ACC/DLPFC activity for high-calorie foods in the NoGo trials under either satiation or deprivation condition negatively correlated with NDSR high-calorie foods (satiety: $r_{45} = -.531, p < .001$; deprivation: $r_{45} = -.572, p < .001$) and BMI (satiety: $r_{45} = -.488, p < .001$; deprivation: $r_{45} = -.612, p < .001$). The insular activity difference between deprivation and satiation conditions was positively correlated with NDSR high-calorie foods (satiety: $r_{45} = .723, p < .001$; deprivation: $r_{45} = .651, p < .001$) and BMI (satiety: $r_{45} = .568, p < .002$; deprivation: $r_{45} = .645, p < .001$). These results suggest that people who consume more high-calorie foods or have higher BMI demonstrate stronger activation of the striatum in response to high-calorie foods, have more difficulty activating the ACC and DLPFC to inhibit automatic responses to high-calorie food, and show higher insular activity when food-deprived.

DCM Results

Starting from a full model, post hoc optimization revealed a sparse model structure at the group level. The sparse structure regarding driving inputs is presented in Table 3, which shows the posterior mean strength and posterior probability for each driving input and each location. Consistent with our hypothesis, Table 3 shows that the left and right striatum were driving input locations for Go trials, the left and right DLPFC and ACC were driving input locations for NoGo trials, and left and right insular activity was driven by deprivation.

The group-level sparse structure regarding modulation effects is shown in Table 4 and Figure 4, which show the posterior mean strength and posterior probability for each modulatory input and each connection. Given the large number of connections ($n = 56$), only connections that had posterior probability of modulation effect greater than .999 are

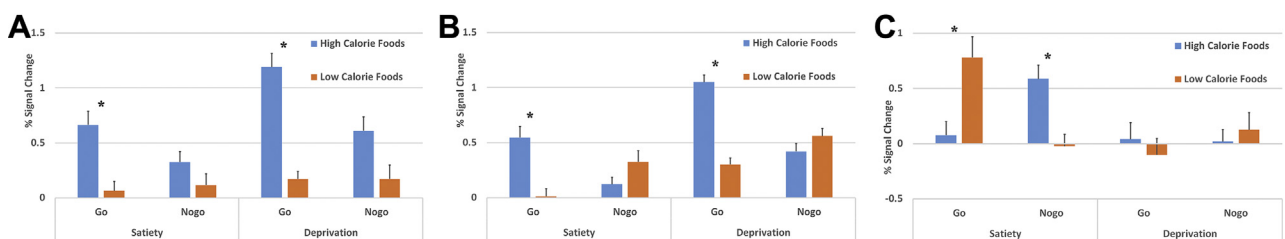


Figure 3. Brain activation pattern illustrated in bar graphs for (A) left striatum, (B) right striatum, and (C) ventromedial prefrontal cortex. The percent signal change for each region was extracted using MarsBaR region of interest toolbox for SPM. Asterisk denotes the significant activation difference between high-calorie foods and low-calorie foods in that condition. Error bars represent SE.

Table 3. Sparse Structure Matrix—Driving Input Effects

Location	Go Trials		NoGo Trials		Deprivation	
	Strength (Hz)	Posterior Probability	Strength (Hz)	Posterior Probability	Strength (Hz)	Posterior Probability
L Striatum	0.0352	.9999	0	0	0	0
R Striatum	0.0323	.9999	0	0	0	0
ACC	0	0	0.0528	.9999	0	0
L DLPFC	0	0	0.0144	.9999	0	0
R DLPFC	0	0	0.0156	.9999	0	0
L Insula	0	0	0	0	0.0022	.9999
R Insula	0	0	0	0	0.0034	.9999
VMPFC	0	0	0	0	0	0

Posterior mean strength (Hz) and posterior probability (77) of each driving input and each driving input location are demonstrated. ACC, anterior cingulate cortex; DLPFC, dorsolateral prefrontal cortex; L, left; R, right; VMPFC, ventromedial prefrontal cortex.

shown in Table 4. Results demonstrated that five connections were modulated by deprivation, including left insula to left DLPFC, right insula to right DLPFC, left insula to left striatum, right insula to right striatum, and right insula to ACC.

The group-level sparse structure regarding the endogenous connections is presented in Table 5, which shows the posterior mean strength and posterior probability of each endogenous connection. Table 5 shows that 19 connections became nonsignificant after post hoc optimization. These include left insula to right DLPFC, left insula to right striatum, left DLPFC to right striatum, left DLPFC to right insula, left DLPFC to ACC, ACC to left DLPFC, ACC to right DLPFC, right insula to left DLPFC, right insula to left striatum, right DLPFC to left DLPFC, right DLPFC to left striatum, right DLPFC to ACC, right DLPFC to left insula, left striatum to ACC, left striatum to right DLPFC, left striatum to right insula, right striatum to ACC, right striatum to left DLPFC, and right striatum to left insula.

The extracted posterior strength of all modulation effects was correlated with BMI and NDSR total scores (combined across the two sessions). The results in Table 4 suggest that all modulation effects were correlated with both BMI and NDSR high-calorie foods except for the modulation of right insula to ACC path, which was not significant after Bonferroni correction.

DISCUSSION

The present study aimed to investigate the network dynamics of three neural systems involved in making food-related choices. Using fMRI and DCM analyses, the results reveal that participants have difficulty inhibiting high-calorie foods when performing a food-specific Go/NoGo task. This behavioral inhibition difficulty is linked to imbalanced activations among three neural systems, with the insula responding to the deprivation state bilaterally, the striatum responding to high-calorie foods bilaterally, and the ACC and DLPFC responding to NoGo trials (i.e., behavioral inhibition attempts). This inhibition difficulty was stronger for participants with higher BMI and for participants who consumed higher calorie foods. DCM analysis showed that food deprivation modulated the connections between the insula, striatum, and DLPFC. These modulations were larger for participants with higher BMI and for participants who consumed higher calorie foods. Altogether, these results provide new insights into the dynamic nature among three neural systems involved in making food-related choices; they also reinforce and extend models that portray the neural mechanism of choices pertaining to other rewarding substances and behaviors (6–8,10,11,12,38,40).

Understanding the underlying neural mechanisms that give rise to food choices that are tempting and rewarding in the short term but can lead to health consequences in the long term can

Table 4. Sparse Matrix Structure—Modulation Effect

Location	Deprivation		Correlated With BMI	Correlated With NDSR High-Calorie Foods
	Strength (Hz)	Posterior Probability		
L Insula → L DLPFC	−0.5647	.9999	$r = -.468, p = .001$	$r = -.711, p < .001$
R Insula → R DLPFC	−0.5273	.9999	$r = -.678, p < .001$	$r = -.672, p < .001$
L Insula → L Striatum	0.7132	.9999	$r = .682, p < .001$	$r = .543, p < .001$
R Insula → R Striatum	0.6950	.9999	$r = .526, p < .001$	$r = .669, p < .001$
R Insula → ACC	−0.3165	.9999	$r = -.317, p = .034^a$	$r = -.308, p = .040^a$

Among the 56 connections, only those that were identified (posterior probability > .999) to be modulated by one of the three conditions are listed. Posterior mean strength (Hz) and posterior probability of each identified (posterior probability > .999) modulation effect are demonstrated.

ACC, anterior cingulate cortex; BMI, body mass index; DLPFC, dorsolateral prefrontal cortex; L, left; NDSR, Nutrition Data System for Research; R, right.

^aNo longer significant after Bonferroni multiple comparison correction.

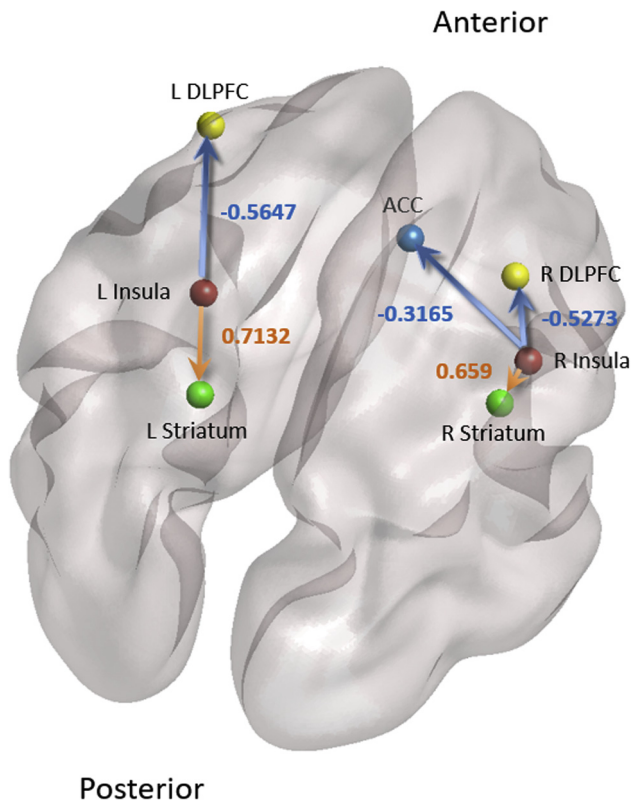


Figure 4. Schematic diagram representing effective connectivity modulated by food deprivation. For clarity, not all nodes are shown. The numbers represent the posterior mean strength (Hz) of the modulation. The positive modulations are shown in orange, and negative modulations are shown in blue. The diagram was visualized with the BrainNet Viewer (76). It was illustrated in a custom view with azimuth = 20 and elevation = 60 to show all brain regions and connections. ACC, anterior cingulate cortex; DLPFC, dorsolateral prefrontal cortex; L, right; R, right.

help inform the development of new therapeutic strategies that potentially improve not only food-related choices but also perhaps other short-term rewarding choices that lead to addictive behaviors. More specifically, the amygdala-striatal (dopamine dependent) neural system (i.e., impulsive system) is critical for the incentive motivational effects of a variety of nonnatural rewards (e.g., psychoactive drugs) and natural rewards (e.g., food) (41). The present study showed that regardless of one's state (satiation or hunger) higher impulsive/habitual system activity is generated in response to high-calorie foods. This is consistent with the idea that the mesolimbic dopamine-striatal system mediates habitual responses to primary reward food cues (42–44). In further support of this notion, functional neuroimaging studies showed that compared with nonfood pictures, food pictures activate the amygdala (45) and the ventral striatum (46) in healthy individuals. It should be noted that the striatum activated in the present study was mostly located in the dorsolateral part in the mid-putamen (right) and posterior (left) putamen. Although studies have shown different roles of ventral and dorsal striatum in response to reward, mounting evidence has suggested that activation of dorsal striatum is common for food-related (13,14,47,48) and other substance-related (49,50) studies. We extend such findings and

show that habitual response in the striatum to high-calorie foods is positively correlated with BMI and NDSR high-calorie food intake. These results are in line with studies showing that food may induce greater incentive values in overweight and obese individuals compared with normal-weight control subjects (51) and in individuals who generally eat more high-calorie foods (13,14) despite other factors that might influence the neural responses to food in overweight and obese individuals (e.g., emotional factors, other psychiatric comorbidities).

Whereas the impulsive system and its related mesolimbic dopamine may explain the drive and seeking of food-related rewards, humans possess decision-making and self-control neural systems that enable them to resist these reward temptations, especially when they lead to long-term negative consequences (12). This decision-making and self-control system has been called the reflective system, and it depends primarily on the functions of the PFC, which is necessary for controlling these more basic motivational drives toward reward and which allows for more flexible pursuit of long-term goals (12). The present study found that the reflective system (and specifically the ACC and DLPFC) was engaged when attempts to control food-related responses were made. We also found that the VMPFC was activated when engaging in inhibitory control, when participants were satiated. This supports extant views regarding the central role of the VMPFC in decision making (52–54) and specifically inhibitory control (55,56). Adequate food-related decision making reflects an integration of both cognitive and affective assessments and the ability to more optimally weigh short-term gains against long-term losses and choose between conflicting alternatives (e.g., consume food now or later). Accordingly, our findings reinforce the role of the VMPFC, ACC, and DLPFC in decision making (12) and extend prior models to the food choice domain.

We also found that the activity of the reflective system was inversely correlated with BMI and NDSR high-calorie food consumption. This finding is in line with previous studies suggesting weaker inhibitory control in overweight and obese individuals (57,58) and individuals who consume more high-calorie foods (3,13,14). It should be noted that we could not conclude that DLPFC plays the same role in obese individuals as normal-weight participants, as in the present study we tested only normal-weight participants. In fMRI studies, it has also been shown that overweight and obese people have less activation in the left DLPFC in response to a meal than their lean counterparts (59). Considering the roles of the impulsive and reflective systems we observed here, our findings lend further support to the idea that excess weight can be explained in part through the lens of decision-making deficits.

The current results also show that the insular cortex is significantly more active in deprivation relative to satiation conditions. Indeed, it has been argued that the insular cortex plays a key role in translating interoceptive signals into what one subjectively experiences as a feeling of desire, anticipation, or urge (12,27). Evidence shows that the insular cortex is also implicated in food craving (47). This is consistent across substances; strokes that damage the insular cortex tend to eliminate the urge to smoke in individuals previously addicted to cigarette smoking (60,61). One proposed mechanism for how this may take place is that activation of interoceptive representations through the insula can, on one hand, sensitize

Table 5. Sparse Matrix Structure—Endogenous Connection

Connection	Strength (Hz)	Posterior Probability	Connection	Strength (Hz)	Posterior Probability
L Striatum → R Striatum	0.0176	.9999	ACC → L Striatum	0.0238	.9999
L Striatum → L DLPFC	0.0159	.9999	ACC → R Striatum	0.0349	.9999
L Striatum → R DLPFC	0.0358	0	ACC → L DLPFC	0.0309	0
L Striatum → ACC	0.0354	0	ACC → R DLPFC	0.0163	0
L Striatum → L Insula	0.0277	.9999	ACC → L Insula	0.0214	.9999
L Striatum → R Insula	0.0320	0	ACC → R Insula	0.0143	.9999
L Striatum → VMPFC	0.0341	.9999	ACC → VMPFC	0.0115	.9999
R Striatum → L Striatum	0.0425	.9999	L Insula → L Striatum	0.0075	.9999
R Striatum → L DLPFC	0.0173	0	L Insula → R Striatum	0.0136	0
R Striatum → R DLPFC	0.0098	.9999	L Insula → L DLPFC	0.0301	.9999
R Striatum → ACC	0.0342	0	L Insula → R DLPFC	0.0346	0
R Striatum → L Insula	0.0144	0	L Insula → ACC	0.0277	.9999
R Striatum → R Insula	0.0371	.9999	L Insula → R Insula	0.0156	.9999
R Striatum → VMPFC	0.0126	.9999	L Insula → VMPFC	0.0231	.9999
L DLPFC → L Striatum	0.0172	.9999	R Insula → L Striatum	0.0104	0
L DLPFC → R Striatum	0.0400	0	R Insula → R Striatum	0.0135	.9999
L DLPFC → R DLPFC	0.0080	.9999	R Insula → L DLPFC	0.0256	0
L DLPFC → ACC	0.0132	0	R Insula → R DLPFC	0.0118	.9999
L DLPFC → L Insula	0.0336	.9999	R Insula → ACC	0.0360	.9999
L DLPFC → R Insula	0.0193	0	R Insula → L Insula	0.0334	.9999
L DLPFC → VMPFC	0.0108	.9999	R Insula → VMPFC	0.0427	.9999
R DLPFC → L Striatum	0.0119	0	VMPFC → L Striatum	0.0162	.9999
R DLPFC → R Striatum	0.0147	.9999	VMPFC → R Striatum	0.0260	.9999
R DLPFC → L DLPFC	0.0173	0	VMPFC → L DLPFC	0.0122	.9999
R DLPFC → ACC	0.0141	0	VMPFC → R DLPFC	0.0082	.9999
R DLPFC → L Insula	0.0169	0	VMPFC → ACC	0.0045	.9999
R DLPFC → R Insula	0.0258	.9999	VMPFC → L Insula	0.0153	.9999
R DLPFC → VMPFC	0.0190	.9999	VMPFC → R Insula	0.0336	.9999

Posterior mean strength (Hz) and posterior probability of each endogenous connection are outlined. ACC, anterior cingulate cortex; DLPFC, dorsolateral prefrontal cortex; L, left; R, right; VMPFC, ventromedial prefrontal cortex.

the impulsive system and, on the other hand, tax the PFC so that it cannot subvert attention, reasoning, planning, and decision-making processes as related to food consumption. Put differently, these interoceptive representations have the capacity to hijack the cognitive resources necessary for exerting inhibitory control to resist calorie-rich food items (12).

Consistent with this idea, the present study demonstrated that the insula triggers changes that alter the dynamic neural balance between the impulsive and reflective systems. This insula-induced modulation of the neural dynamics was larger in participants with higher BMI and in participants who eat more high-calorie foods. These results extend several neuroimaging studies showing that food versus nonfood pictures activate the insular cortex in healthy individuals (62,63). The increased activity induced by food presentation in the insular cortex significantly correlated with self-reports of hunger and desire for food in normal-weight subjects (47,64). One recent fMRI study (65) reported that compared with lean adolescent girls, obese girls showed greater activation in the gustatory cortex (anterior insula and mid-insula and frontal operculum) and in somatosensory regions (parietal operculum and Rolandic operculum) in response to the anticipated intake of a chocolate milkshake (vs. a tasteless solution) and to actual

consumption of a milkshake (vs. a tasteless solution). Another recent study examined resting-state functional connectivity difference of the dorsal mid-insula both before and after a meal; the findings suggested obesity-related alterations in dorsal mid-insula functional connectivity patterns (66). Overall, our results provide further evidence regarding the centrality of the insular system in decision making and extend this perspective to show how the insula dynamically modulates neural processes that govern food-related behaviors.

Several limitations of this study are noteworthy. First, the sample included presumably healthy individuals with normal weights. Although our study suggested that the individual differences of DCM networks were correlated with BMI and in line with a previous report suggesting insular functional connectivity difference between obese and normal-weight participants (66), we could not extend our inferences to clinically obese people or people with higher BMI. Second, the generalization of conclusion to female subjects may be influenced by the phase of menstrual cycle because there are studies suggesting reward processing by women (67,68), including food cues processing (69,70), is influenced by the phase of menstrual cycle and oral contraceptive use (71). Third, we did not find a significant interaction between condition and task. This might be an artifact

of the sample (healthy young individuals) and/or the task condition (unfamiliar fMRI environment). Nevertheless, such nonsignificant differences might also suggest that groups were matched on task difficulty, making fMRI difference more prominent. Fourth, the main conclusion were drawn from the DCM results. Nevertheless, it is debated if fMRI signals could be used for casual inference because of the time lag that limits the accuracy of causal modeling with fMRI data (72,73). Lastly, we could not fully enforce deprivation and satiation. We did not measure or actually control how much participants consumed before the scans. While hunger was indeed higher in the deprivation condition, future studies may replicate ours in a controlled environment where food intake (or lack of in deprivation condition) could be fully controlled by the researchers.

Ultimately, our results portray a tripartite model of key neural systems that govern food-related choices. This is consistent with the recent literature that supports the idea of an overlap between the neural systems underlying drug-seeking behaviors and eating high-calorie food (6,11,74). The findings advance our understanding of excess weight, possibly extended to obesity, especially of food choices in adolescents who have underdeveloped PFC (75) and in environments such as school or university campuses where unhealthy food options are prominent.

ACKNOWLEDGMENTS AND DISCLOSURES

This work was supported by the National Natural Science Foundation of China (Grant No. 31400959 [to QH]), Entrepreneurship and Innovation Program for Chongqing Overseas Returned Scholars (Grant No. cx2017049 [to QH]), Fundamental Research Funds for Central Universities (Grant Nos. SWU1809003 and SWU1709106 [to QH]), National Institute on Drug Abuse (Grant No. R01DA023051 [to AB]), National Cancer Institute (Grant No. R01CA152062 [to AB]), and National Heart, Lung, and Blood Institute and National Institute of Child Health and Human Development (Grant No. U01HL097839 [to AB]).

QH, OT, and AB designed the study. QH collected the data. QH, XH, SZ, OT, and LM analyzed the data. QH, XH, SZ, OT, LM, and AB wrote the manuscript. All authors approved the final version of the manuscript.

The authors report no biomedical financial interests or potential conflicts of interest.

ARTICLE INFORMATION

From the Faculty of Psychology (QH, XH), Southwest University; Chongqing Collaborative Innovation Center for Brain Science (QH); Southwest University Branch (QH), Collaborative Innovation Center of Assessment toward Basic Education Quality, Beibei, Chongqing; Faculty of Education (SZ), Guangxi Normal University, Guangxi Colleges and Universities Key Laboratory of Cognitive Neuroscience and Applied Psychology, Guilin, Guangxi, China; Information Systems and Decision Sciences (OT), California State University, Fullerton; Brain and Creativity Institute (OT, AB) and Department of Psychology (OT, AB), University of Southern California, Los Angeles, California; Department of Radiology (LM), Virginia Commonwealth University, and Institute for Drug and Alcohol Studies (LM), Richmond, Virginia.

Address correspondence to Qinghua He, Ph.D., Faculty of Psychology, Southwest University, No. 2 Tiansheng Road, Beibei, Chongqing 400715, China; E-mail: heqinghua@swu.edu.cn.

Received Nov 6, 2018; accepted Dec 5, 2018.

Supplementary material cited in this article is available online at <https://doi.org/10.1016/j.bpsc.2018.12.005>.

REFERENCES

- Stein CJ, Colditz GA (2004): The epidemic of obesity. *J Clin Endocrinol Metab* 89:2522–2525.
- Wang Y, Mi J, Shan XY, Wang QJ, Ge KY (2007): Is China facing an obesity epidemic and the consequences? The trends in obesity and chronic disease in China. *Int J Obes (Lond)* 31:177–188.
- He Q, Chen C, Dong Q, Xue G, Chen C, Lu Z, *et al.* (2015): Gray and white matter structures in the midcingulate cortex region contribute to body mass index in Chinese young adults. *Brain Struct Funct* 220:319–329.
- Rehman AG, Tyson M, Egger M, Heller RF, Zwahlen M (2008): Body-mass index and incidence of cancer: A systematic review and meta-analysis of prospective observational studies. *Lancet* 371:569–578.
- Weiss R, Dziura J, Burgert TS, Tamborlane WV, Taksali SE, Yeckel CW, *et al.* (2004): Obesity and the metabolic syndrome in children and adolescents. *N Engl J Med* 350:2362–2374.
- Volkow ND, Baler RD (2015): NOW vs LATER brain circuits: Implications for obesity and addiction. *Trends Neurosci* 38:345–352.
- Volkow ND, Wang GJ, Fowler JS, Telang F (2008): Overlapping neuronal circuits in addiction and obesity: Evidence of systems pathology. *Philos Trans R Soc Lond B Biol Sci* 363:3191–3200.
- Kelley AE, Berridge KC (2002): The neuroscience of natural rewards: Relevance to addictive drugs. *J Neurosci* 22:3306–3311.
- Rolls E (2007): Understanding the mechanisms of food intake and obesity. *Obes Rev* 8:67–72.
- Trinko R, Sears RM, Guarnieri DJ, DiLeone RJ (2007): Neural mechanisms underlying obesity and drug addiction. *Physiol Behav* 91:499–505.
- Volkow ND, Wise RA (2005): How can drug addiction help us understand obesity? *Nat Neurosci* 8:555–560.
- Noël X, Brevers D, Bechara A (2013): A neurocognitive approach to understanding the neurobiology of addiction. *Curr Opin Neurobiol* 23:632–638.
- He Q, Xiao L, Xue G, Wong S, Ames SL, Bechara A (2014): Altered dynamics between neural systems sub-serving decisions for unhealthy food. *Front Neurosci* 8:350.
- He Q, Xiao L, Xue G, Wong S, Ames SL, Schembre SM, *et al.* (2014): Poor ability to resist tempting calorie rich food is linked to altered balance between neural systems involved in urge and self-control. *Nutr J* 13:92.
- Bechara A (2005): Decision making, impulse control and loss of will-power to resist drugs: A neurocognitive perspective. *Nat Neurosci* 8:1458–1463.
- Bechara A, Van Der Linden M (2005): Decision-making and impulse control after frontal lobe injuries. *Curr Opin Neurol* 18:734–739.
- Crews FT, Boettiger CA (2009): Impulsivity, frontal lobes and risk for addiction. *Pharmacol Biochem Behav* 93:237–247.
- Cao F, Su L, Liu T, Gao X (2007): The relationship between impulsivity and Internet addiction in a sample of Chinese adolescents. *Eur Psychiatry* 22:466–471.
- Kim SM, Huh HJ, Cho H, Kwon M, Choi JH, Ahn HJ, *et al.* (2014): The effect of depression, impulsivity, and resilience on smartphone addiction in university students. *J Korean Neuropsychiatr Assoc* 53:214–220.
- Kreek MJ, Nielsen DA, Butelman ER, LaForge KS (2005): Genetic influences on impulsivity, risk taking, stress responsivity and vulnerability to drug abuse and addiction. *Nat Neurosci* 8:1450.
- Ghahremani DG, Lee B, Robertson CL, Tabibnia G, Morgan AT, De Shetler N, *et al.* (2012): Striatal dopamine D2/D3 receptors mediate response inhibition and related activity in frontostriatal neural circuitry in humans. *J Neurosci* 32:7316–7324.
- Lee B, London ED, Poldrack RA, Farahi J, Nacca A, Monterosso JR, *et al.* (2009): Striatal dopamine D2/D3 receptor availability is reduced in methamphetamine dependence and is linked to impulsivity. *J Neurosci* 29:14734–14740.
- Craig AD (2009): How do you feel—now? The anterior insula and human awareness. *Nat Rev Neurosci* 10:59–70.
- Craig A (2011): Significance of the insula for the evolution of human awareness of feelings from the body. *Ann N Y Acad Sci* 1225:72–82.
- Craig A (2009): Emotional moments across time: A possible neural basis for time perception in the anterior insula. *Philos Trans R Soc Lond B Biol Sci* 364:1933–1942.
- Craig A (2003): Interoception: The sense of the physiological condition of the body. *Curr Opin Neurobiol* 13:500–505.
- Droutman V, Read SJ, Bechara A (2015): Revisiting the role of the insula in addiction. *Trends Cogn Sci* 19:414–420.

Insula and Food Reward

28. Friston KJ, Harrison L, Penny W (2003): Dynamic causal modelling. *Neuroimage* 19:1273–1302.
29. Wechsler D (1999): Wechsler Abbreviated Scale of Intelligence. New York, NY: The Psychological Corporation.
30. Cragg L, Nation K (2007): Self-ordered pointing as a test of working memory in typically developing children. *Memory* 15:526–535.
31. Feskanich D, Sietaff BH, Chong K, Buzzard IM (1989): Computerized collection and analysis of dietary intake information. *Comput Methods Programs Biomed* 30:47–57.
32. Johnson RK, Driscoll P, Goran MI (1996): Comparison of multiple-pass 24-hour recall estimates of energy intake with total energy expenditure determined by the doubly labeled water method in young children. *J Am Diet Assoc* 96:1140.
33. Turel O, He Q, Xue G, Xiao L, Bechara A (2014): Examination of neural systems sub-serving Facebook “addiction.” *Psychol Rep* 115:675–695.
34. Simmonds DJ, Pekar JJ, Mostofsky SH (2008): Meta-analysis of Go/No-go tasks demonstrating that fMRI activation associated with response inhibition is task-dependent. *Neuropsychologia* 46:224–232.
35. Swick D, Ashley V, Turken U (2011): Are the neural correlates of stopping and not going identical? Quantitative meta-analysis of two response inhibition tasks. *Neuroimage* 56:1655–1665.
36. Turel O, Bechara A (2016): A triadic reflective-impulsive-interoceptive awareness model of general and impulsive information system use: Behavioral tests of neuro-cognitive theory. *Front Psychol* 7:1–11.
37. Ma L, Steinberg JL, Cunningham KA, Lane SD, Kramer LA, Narayana PA, *et al.* (2015): Inhibitory behavioral control: A stochastic dynamic causal modeling study using network discovery analysis. *Brain Connect* 5:177–186.
38. Stephan KE, Penny WD, Moran RJ, den Ouden HE, Daunizeau J, Friston KJ (2010): Ten simple rules for dynamic causal modeling. *Neuroimage* 49:3099–3109.
39. Friston KJ, Li B, Daunizeau J, Stephan KE (2011): Network discovery with DCM. *Neuroimage* 56:1202–1221.
40. Sowell ER, Peterson BS, Thompson PM, Welcome SE, Henkenius AL, Toga AW (2003): Mapping cortical change across the human life span. *Nat Neurosci* 6:309–315.
41. Wise RA (2002): Brain reward circuitry: Insights from unsensed incentives. *Neuron* 36:229–240.
42. Siep N, Roefs A, Roebroek A, Havermans R, Bonte ML, Jansen A (2009): Hunger is the best spice: An fMRI study of the effects of attention, hunger and calorie content on food reward processing in the amygdala and orbitofrontal cortex. *Behav Brain Res* 198:149–158.
43. Ng J, Stice E, Yokum S, Bohon C (2011): An fMRI study of obesity, food reward, and perceived caloric density. Does a low-fat label make food less appealing? *Appetite* 57:65–72.
44. Grill HJ, Skibicka KP, Hayes MR (2007): Imaging obesity: fMRI, food reward, and feeding. *Cell Metab* 6:423–425.
45. Gottfried JA, O’Doherty J, Dolan RJ (2003): Encoding predictive reward value in human amygdala and orbitofrontal cortex. *Science* 301:1104–1107.
46. Morris J, Dolan R (2001): Involvement of human amygdala and orbitofrontal cortex in hunger-enhanced memory for food stimuli. *J Neurosci* 21:5304–5310.
47. Pelchat ML, Johnson A, Chan R, Valdez J, Ragland JD (2004): Images of desire: Food-craving activation during fMRI. *Neuroimage* 23:1486–1493.
48. Rothmund Y, Preuschhof C, Böhner G, Bauknecht HC, Klingebiel R, Flor H, *et al.* (2007): Differential activation of the dorsal striatum by high-calorie visual food stimuli in obese individuals. *Neuroimage* 37:410–421.
49. Volkow ND, Wang GJ, Telang F, Fowler JS, Logan J, Childress AR, *et al.* (2006): Cocaine cues and dopamine in dorsal striatum: Mechanism of craving in cocaine addiction. *J Neurosci* 26:6583–6588.
50. McClernon FJ, Kozink RV, Lutz AM, Rose JE (2009): 24-h smoking abstinence potentiates fMRI-BOLD activation to smoking cues in cerebral cortex and dorsal striatum. *Psychopharmacology* 204:25–35.
51. Temple JL, Legierski CM, Giacomelli AM, Salvy SJ, Epstein LH (2008): Overweight children find food more reinforcing and consume more energy than do nonoverweight children. *Am J Clin Nutr* 87:1121–1127.
52. Bechara A, Tranel D, Damasio H, Damasio AR (1996): Failure to respond autonomically to anticipated future outcomes following damage to prefrontal cortex. *Cereb Cortex* 6:215–225.
53. Bechara A, Damasio H, Tranel D, Damasio AR (1997): Deciding advantageously before knowing the advantageous strategy. *Science* 275:1293–1295.
54. Bechara A, Damasio H, Tranel D, Anderson SW (1998): Dissociation of working memory from decision making within the human prefrontal cortex. *J Neurosci* 18:428–437.
55. Aron AR, Fletcher PC, Bullmore ET, Sahakian BJ, Robbins TW (2003): Stop-signal inhibition disrupted by damage to right inferior frontal gyrus in humans. *Nat Neurosci* 6:115–116.
56. Aron A, Robbins T, Poldrack R (2004): Inhibition and the right inferior frontal cortex. *Trends Cogn Sci* 8:170–177.
57. Nederkoom C, Braet C, Van Eijs Y, Tanghe A, Jansen A (2006): Why obese children cannot resist food: The role of impulsivity. *Eat Behav* 7:315–322.
58. Loeber S, Grosshans M, Korucuoglu O, Vollmert C, Vollstädt-Klein S, Schneider S, *et al.* (2012): Impairment of inhibitory control in response to food-associated cues and attentional bias of obese participants and normal-weight controls. *Int J Obes* 36:1334–1339.
59. Le DSN, Pannacciulli N, Chen K, Del Parigi A, Salbe AD, Reiman EM, *et al.* (2006): Less activation of the left dorsolateral prefrontal cortex in response to a meal: A feature of obesity. *Am J Clin Nutr* 84:725–731.
60. Naqvi NH, Rudrauf D, Damasio H, Bechara A (2007): Damage to the insula disrupts addiction to cigarette smoking. *Science* 315:531–534.
61. Naqvi NH, Bechara A (2009): The hidden island of addiction: The insula. *Trends Neurosci* 32:56–67.
62. Frank S, Laharnar N, Kullmann S, Veit R, Canova C, Hegner YL, *et al.* (2010): Processing of food pictures: Influence of hunger, gender and calorie content. *Brain Res* 1350:159–166.
63. Simmons WK, Martin A, Barsalou LW (2005): Pictures of appetizing foods activate gustatory cortices for taste and reward. *Cerebral Cortex* 15:1602–1608.
64. Schienle A, Schäfer A, Hermann A, Vaitl D (2009): Binge-eating disorder: Reward sensitivity and brain activation to images of food. *Biol Psychiatry* 65:654–661.
65. Small DM, Zatorre RJ, Dagher A, Evans AC, Jones-Gotman M (2001): Changes in brain activity related to eating chocolate. *Brain* 124:1720–1733.
66. Avery JA, Powell JN, Breslin FJ, Lepping RJ, Martin LE, Patricia TM, *et al.* (2017): Obesity is associated with altered mid-insula functional connectivity to limbic regions underlying appetitive responses to foods. *J Psychopharmacol* 31:1475–1484.
67. Berns GS, McClure SM, Pagnoni G, Montague PR (2001): Predictability modulates human brain response to reward. *J Neurosci* 21:2793–2798.
68. Dreher JC, Schmidt PJ, Kohn P, Furman D, Rubinov D, Berman KF (2007): Menstrual cycle phase modulates reward-related neural function in women. *Proc Natl Acad Sci U S A* 104:2465–2470.
69. Van Vugt DA (2009): Brain imaging studies of appetite in the context of obesity and the menstrual cycle. *Hum Reprod Update* 16:276–292.
70. Frank TC, Kim GL, Krzemien A, Van Vugt DA (2010): Effect of menstrual cycle phase on corticolimbic brain activation by visual food cues. *Brain Res* 1363:81–92.
71. De Silva A, Salem V, Long CJ, Makwana A, Newbould RD, Rabiner EA, *et al.* (2011): The gut hormones PYY3-36 and GLP-17-36 amide reduce food intake and modulate brain activity in appetite centers in humans. *Cell Metab* 14:700–706.
72. Ramsey JD, Hanson SJ, Hanson C, Halchenko YO, Poldrack RA, Glimmour C (2010): Six problems for causal inference from fMRI. *Neuroimage* 49:1545–1558.
73. Smith SM (2012): The future of fMRI connectivity. *Neuroimage* 62:1257–1266.
74. Wang GJ, Volkow ND, Telang F, Jayne M, Ma J, Rao M, *et al.* (2004): Exposure to appetitive food stimuli markedly activates the human brain. *Neuroimage* 21:1790–1797.
75. Giedd J, Blumenthal J, Jeffries N, Castellanos F, Liu H, Zijdenbos A, *et al.* (1999): Brain development during childhood and adolescence: A longitudinal MRI study. *Nature Neurosci* 2:861–862.
76. Xia M, Wang J, He Y (2013): BrainNet Viewer: A network visualization tool for human brain connectomics. *PLoS One* 8:e68910.
77. Seghier ML, Friston KJ (2013): Network discovery with large DCMs. *Neuroimage* 68:181–191.